Using Satellite Radiation Measurements for Model Evaluation

J.-J. Morcrette[1], F. Chevallier[1], J.-C. Buriez[2], and F. Hennequart[2]

[1]E.C.M.W.F., Shinfield Park, Reading Berkshire, RG2 9AX, United Kingdom

[2]Laboratoire d'Optique Atmospherique, U.S.T.L., 59655 - Villeneuve d'Ascq Cedex, France

1. Introduction

In the context of numerical weather forecasting, the parametrizations responsible for producing the clouds and associated radiative fields were, for years, only questioned when meteorological parameters such as the temperature, within the atmosphere, or at the surface, were displaying a bias relative to the analyzed temperature profiles, or to the observations of the temperature at two metres. Precipitation was also produced independently from the clouds, through large-scale condensation or convective processes, with almost no relation to the state of cloudiness. Profiles of cloud fraction and cloud water were then produced using diagnostic relationships (*Slingo*, 1987) linking those parameters to the relative humidity, with filters on vertical velocity and potential temperature gradient in an effort to represent boundary-layer clouds, or to the convective precipitation for representing the convective clouds and associated anvils. A study of the diurnal cycle of the model cloudiness as diagnosed from radiances simulated from the model fields (*Morcrette*, 1991) was one among other studies indicating the limited success of the model at representing the four-dimensional distribution of the cloudiness and cloud water at that time.

In 1995, the introduction in the ECMWF model, of a cloud scheme (*Tiedtke*, 1993) with two prognostic equations for cloud amount and cloud water, shifted the emphasis, and more diagnostic studies have since been related to an evaluation of the quality of the clouds, particularly of the cloud cover and height (*Jakob*, 1999; *Klein and Jakob*, 1999). However, in a weather forecast context, the overall limited number of such studies, in the past, is mainly explained by the fact that, only the so-called cleared radiances are operationally used in the analyses, out of radiance data sets, measured either from polar-orbiting or geostationary satellites, that originally include also cloudy radiances.

In the development of physical parametrizations, climatologies of clouds and radiation fields, such as ISCCP, ERBE, have been used, over the years, but mainly for checking the long-term behaviour of the model, in seasonally-long simulations. However, in an operational environment such as ECMWF's, the time-scales over which such a validation should be conducted is quite large, from instantaneous snapshots

to be compared to satellite imagery, to the 12-hour span of the first-guess forecasts used to create the background fields over which the analysis is performed, to the length of the operational forecasts (presently 10-day long at ECMWF), and to the several months encompassed by seasonal forecasts.

Here we briefly report some recent efforts at using new satellite datasets to (in)validate the present representation of the clouds and related radiation fields at the top of the atmosphere. In section 2, we first look at the monthly time-scale and the impact on the top-of-the-atmosphere (TOA) radiation of the recent change of longwave radiation scheme. The representation of the diurnal cycle following the methodology of *Morcrette* (1991) is revisited in Section 3. Brightness temperatures, observed and simulated, are also considered in Section 4, but in terms of the spectral signature of the clouds in the longwave channels of the GOES-8 geostationary satellite. In section 5, using parameters derived from instantaneous observations from ADEOS-POLDER, we assess the model cloud optical thickness in the shortwave part of the spectrum and its spatial variability.

2. Monthly-mean longwave radiation at the top of the atmosphere

ECMWF is responsible for operational analyses of meteorological data, 10-day forecasts at high spatial resolution (at the time of the Seminar, T_L319 L60, i.e., a physical grid of roughly $[0.5625 \text{ deg}]^2$, with levels from the surface to 0.2 hPa) and seasonal forecasts. In the forecast model, the package of physical parametrizations was upgraded in September 1999 then in June 2000, and now includes a new surface scheme (*van den Hurk et al.*, 2000) and the Rapid Radiation Transfer Model. RRTM is a longwave radiation transfer scheme developed by *Mlawer et al.* (1997), with an accuracy equivalent to that of the line-by-line model from which it was developed. It replaced the longwave radiation scheme of *Morcrette* (1990) (hereafter M'90). A new precipitation scheme (*Jakob and Klein*, 2000) accounts for the overlap between cloud layers when computing the evaporation of the falling precipitation.

To check the outgoing longwave radiation (OLR) at TOA produced by the ECMWF model, we use here the monthly averaged OLR derived from HIRS/2 measurements by NCEP CDC. The OLR is produced with the help of a regression analysis originally proposed by *Ellingson and Ferraro* (1983) and refined hereafter (*Ellingson et al.*, 1994), using several HIRS/2 channel radiances from NOAA-14. A similar study for July 1998 using CERES data and a previous version of the ECMWF model was recently published by *Chevallier and Morcrette* (2000).

Figure 1 presents the monthly averaged OLR derived from HIRS/2 radiances by NCEP-CDC, and the corresponding fields derived either from the RRTM- or the M'90 forecasts during the first 24 hours of integration. While the gross features of the OLR are properly represented by the ECMWF model, a number of local deficiencies are also apparent: the too large OLR over equatorial Africa, north of South Amer

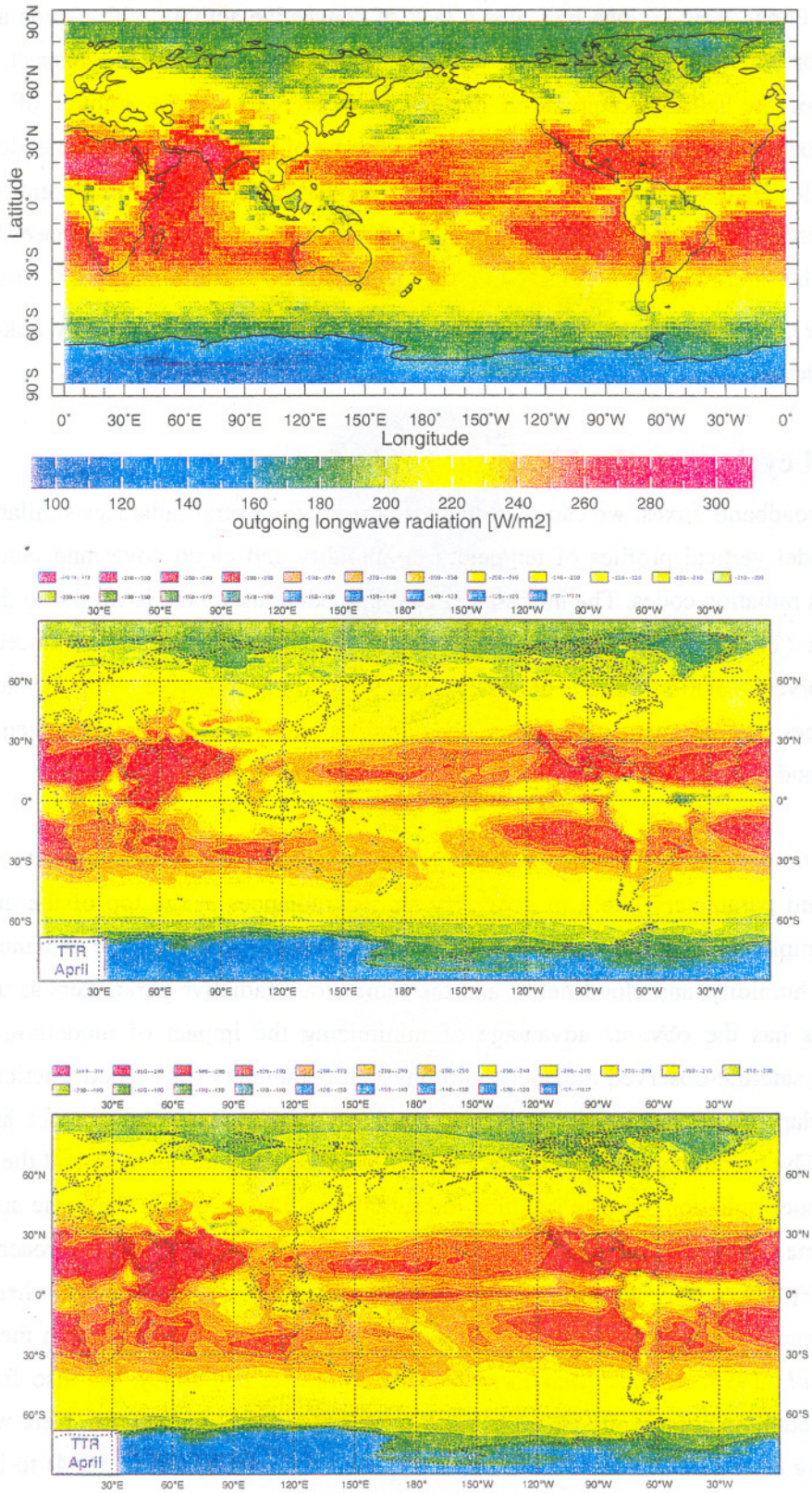

Figure 1: The outgoing longwave radiation at the top of the atmosphere for April 2000, as derived from HIRS/2 radiances by NCEP-CDC (top), and as described in the 30 x 24-hour forecasts with the ECMWF forecast system

Borneo, and Papua New Guinea indicates a lack of convective activity with clouds not penetrating high enough and/or with too little condensed water in their upper extent. In this respect, the revision of the evaporation of the falling precipitation has led to a decrease in the amount of cloud water, partly responsible for the overestimation of the OLR. Over some of the desert areas of the globe, the model gives slightly smaller OLR (Sahara, Arabian Peninsula, Pakistan). However, at this point, part of the problem might be linked to the retrieval of OLR from HIRS/2 observations and potential biases linked to the diurnal coverage of the satellite observations (NOAA-14 has a 13:30 Z ascending mode). At the other extreme of the range, the OLR over the Antarctica plateau is too high by 10 Wm^{-2}, certainly linked to too few or too transparent clouds.

3. Diurnal cycle over the Meteosat field-of-view

As well as broadband fluxes, we can also diagnose (narrow) spectral radiances similar to the observations from the model vertical profiles of temperature, humidity and cloud cover and cloud condensed water using various radiation codes. The intercomparison procedure used here is similar to the original approach by *Morcrette* (1991). When attempting to validate the cloud distribution produced by a model with satellite-observed radiation fields, one can try, as in Section 5, to derive cloud physical parameters from these radiances and compare with the same model parameters (e.g., cloud condensates, cloud optical thickness, cloud effective radius, cloud top height, cloud fractional cover).

Most of the time, with the radiance data set (such as ISCCP), there usually exists a large ensemble of differing cloud parameters likely to give very similar radiances at the top of the atmosphere. Another approach completely bypasses such a retrieval and produces satellite-type radiances from the model temperature, humidity, and cloud fields, and the same cloud radiative parameters as used in the radiation scheme. This has the obvious advantage of minimizing the impact of modelling assumptions when transforming satellite-observed radiances into physical parameters (i.e., cloud fractional cover and cloud vertical overlap, cloud top height and/or temperature, condensed water content and cloud longwave emissivity). The modelling assumptions are basically only on the model side, and the only difficulty is to make the model radiation scheme produce the satellite radiances within the same spectral channels and under the same geometry as the observations. Over the recent years, such an approach has recruited more and more adepts, not only within the operational weather forecast community where the simulation of satellite radiances from model variables is at the core of variational assimilation methods (*Rikus*, 1997; *Saunders et al.*, 1999; *Mahfouf and Rabier*, 2000; *Rabier et al.*, 2000), but also from the climate and mesoscale modelling community (*Roca et al.*, 1997; *Chaboureau et al.*, 2000). Here we use the RTTOV-6 package (*Eyre et al.*, 1990; *Saunders et al.*, 1999) first modified by *Rizzi* (1994) to include not the one-layer effective cloud of the original scheme, but the effect on the outgoing radiance of a vertical distribution of effective cloud layers following the approach of *Washington and Williamson* (1977) also

used in the ECMWF model radiation scheme. This package was recently further upgraded by *Chevallier et al.* (2000) to replace these effective cloud layers by a more proper treatment of the semi-transparent clouds using the true fractional cloud cover and layer emissivity following *Raisanen* (1998). In the following, this so-called "cloudy" RTTOV-6 package is used to simulate the radiances in various parts of the longwave spectrum. They are then compared to the corresponding radiances measured by different geostationary satellites.

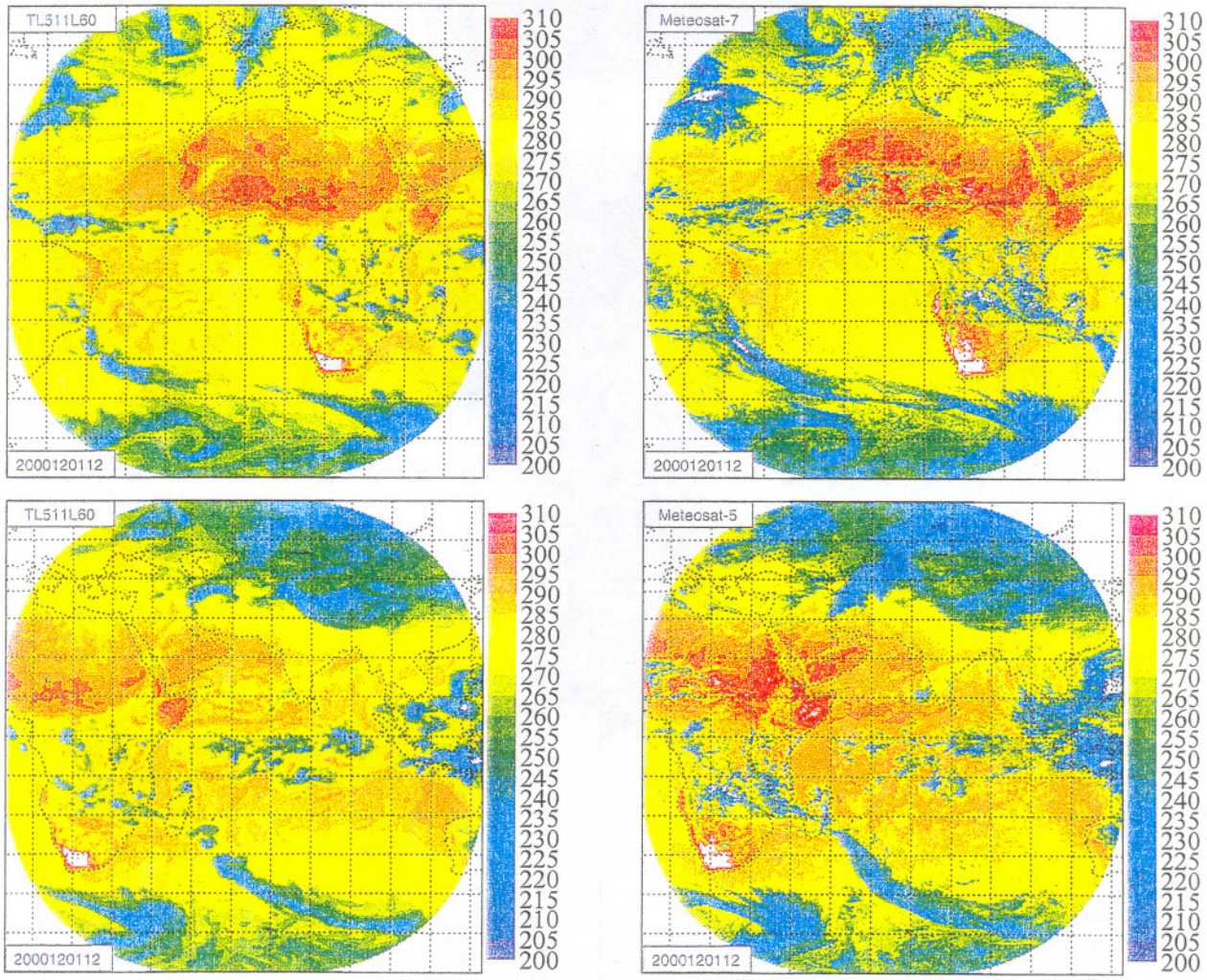

Figure 2: The longwave window channel brightness temperature (in Kelvins) simulated from the model fields (left panels) and observed by the geostationary satellites for the 20001201 12UTC. Top pictures are for the Meteosat-7 satellite over 0°, bottom pictures are for the Meteosat-5 satellite over 63° E.

Figures 2 compare the model to the Meteosat-7 (over Africa) and Meteosat-5 (over the Indian ocean) 11 μm observations for 20001201 12UTC. The model is reasonably successful in its representation of the mid to high-level cloudiness that really impact the TOA brightness temperatures. Most of the main cloud systems are properly located. The only missing feature is the streak of cirriform clouds across the Sahara.

Overall the brightness temperature through these high clouds is usually overestimated by the model, with clouds either absent, not high or not optically thick enough.

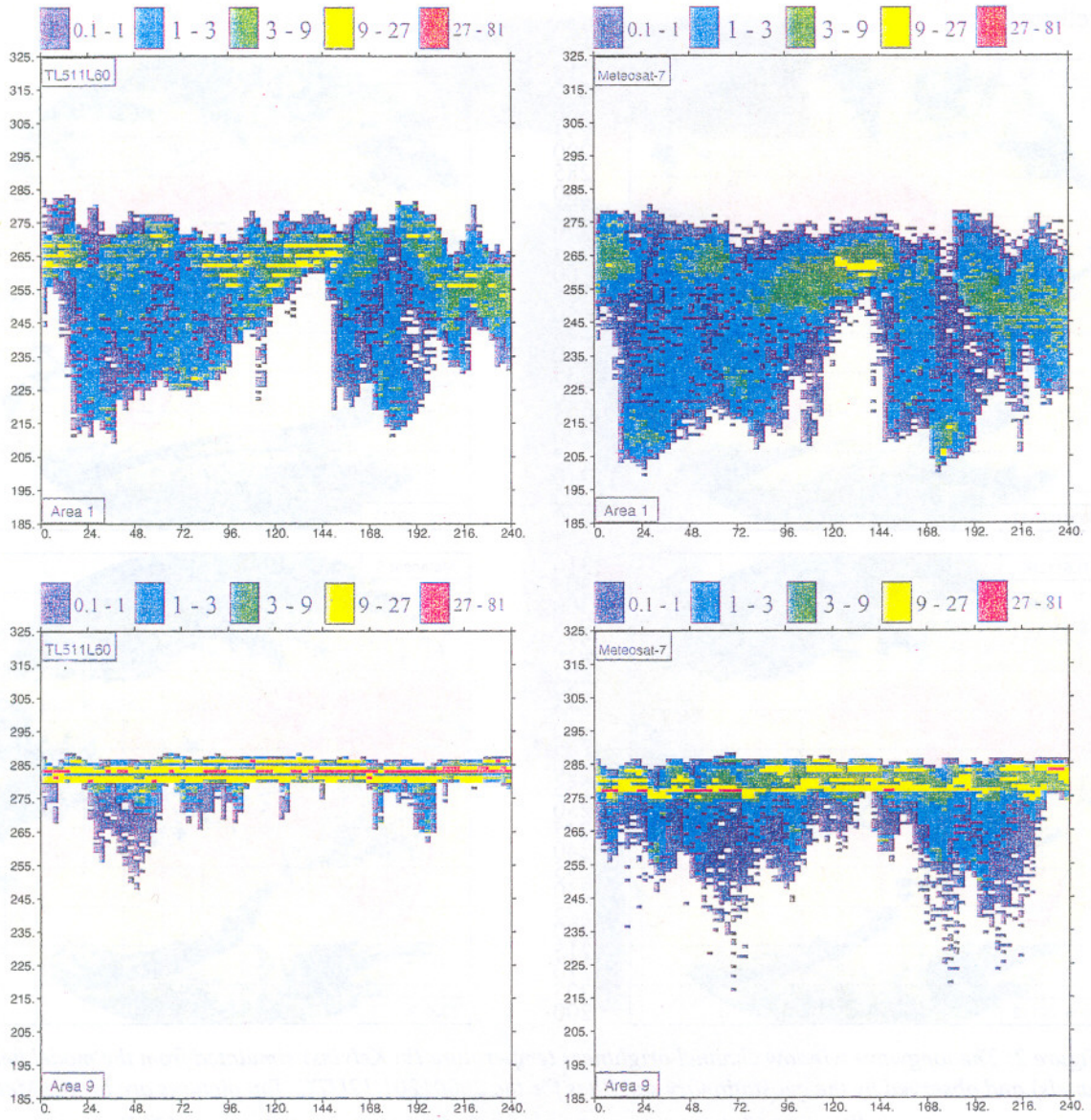

Figure 3: The evolution histogram of the longwave window brightness temperature over the Newfoundland Basin (top) and the area Off-Coast Angola (bottom). Model is on the left, Meteosat-7 observations are on the right. Colour coding is related to the fraction of pixels in 1 K intervals within the 185-325 K temperature range. Evolution histograms are built from brightness temperatures, either simulated or observed every 3 hours during the period 20001201 00UTC to 20001211 00UTC.

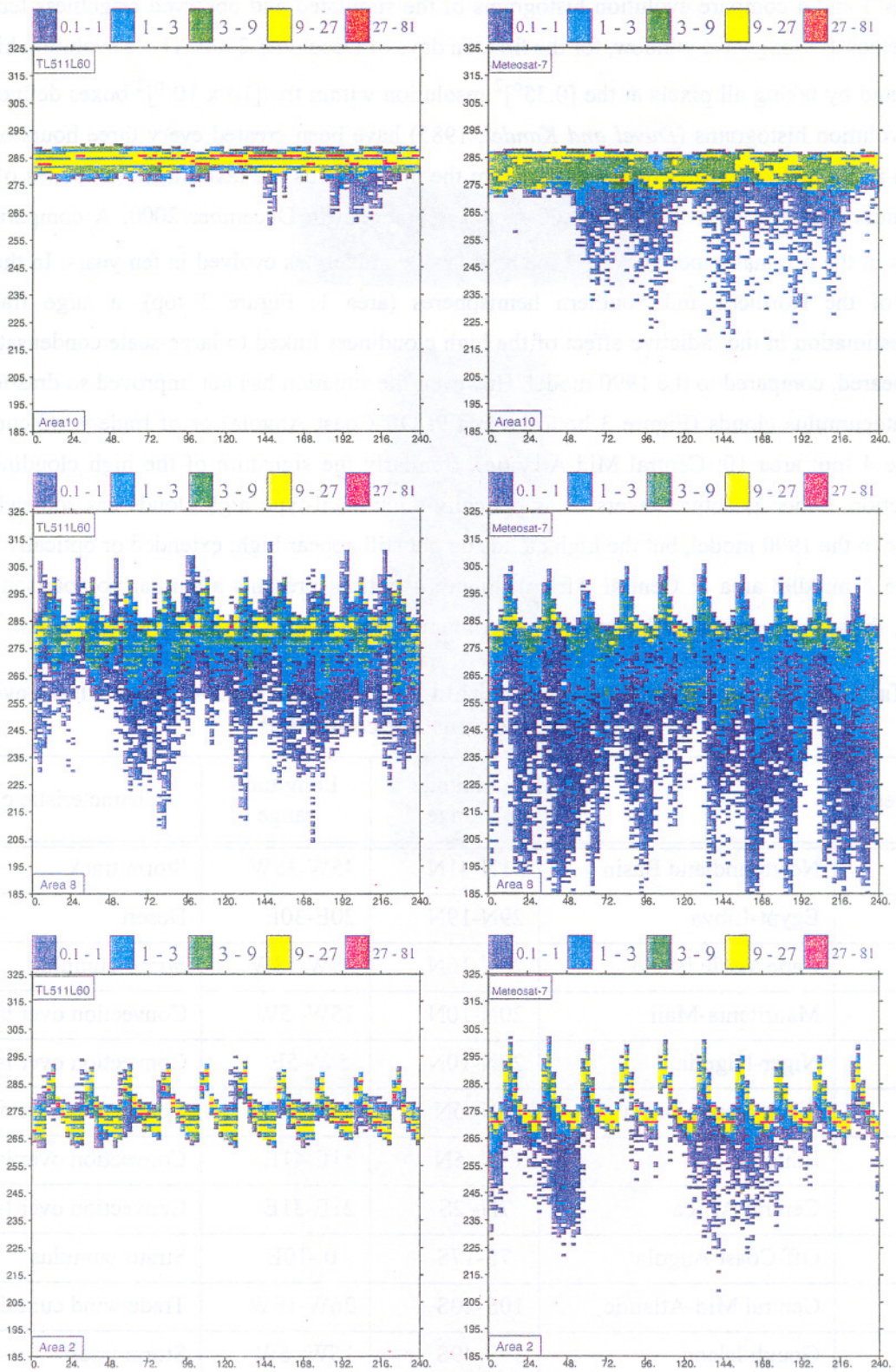

Figure 4: As in Figure 3, but for the Central Mid-Atlantic area (top), the Central Africa area (middle) and the Egypt-Lybia area (bottom).

Figures 3 and 4 compare evolution histograms of the simulated and observed brightness temperatures in the Meteosat-7 longwave window, for the first ten days of December 2000. These evolution histograms are computed by taking all pixels at the $[0.35^{o}]^2$ resolution within the $[10 \times 10\ ^{o}]^2$ boxes defined in Table 1. The evolution histograms (*Duvel and Kandel*, 1985) have been created every three hours over the same eleven areas studied in *Morcrette* (1991). Here the model fields are taken from the series of the 12-hour first-guess forecasts with the T_L511L60 model operational in December 2000. A comparison with the figures in the original paper allows to see how far the model has evolved in ten years. In the storm track areas of the Northern and Southern hemispheres (area 1: Figure 3 top), a large fraction of the underestimation in the radiative effect of the high cloudiness linked to large-scale condensation, has now disappeared, compared to the 1990 model. However, the situation has not improved so drastically in areas of stratocumulus clouds (Figure 3 bottom: area 9: Off-Coast Angola) or of trade-wind cumulus clouds (Figure 4 top: area 10: Central Mid-Atlantic). Similarly the signature of the high cloudiness linked to convection, either as active towers or as optically thick anvil-type high clouds has somewhat improved relative to the 1990 model, but the high clouds do not still appear high, extended or optically thick enough (Figure 4 middle: area 8: Central Africa). Figure 4 bottom presents a similar comparison over Egypt-Libya, showing the model with a too cold maximum surface temperature around local noon.

Table 1: The eleven limited areas within the Meteosat field-of-view where evolution histograms are computed

Area		Latitude range	Longitude range	Characteristic cloud type
1	Newfoundland Basin	51N-41N	45W-35W	Storm track
2	Egypt-Libya	29N-19N	20E-30E	Desert
3	Cape Verde Island	26N-16N	28W-18W	Strato-cumulus
4	Mauritania-Mali	20N-10N	15W- 5W	Convection over land
5	Niger-Nigeria	20N-10N	5W- 5E	Convection over land
6	Sierra Leone Basin	16N- 6N	33W-23W	Convection over ocean
7	Ethiopia	15N- 5N	31E-41E	Convection over land
8	Central Africa	7N- 2S	21E-31E	Convection over land
9	Off-Coast Angola	7S-17S	0 -10E	Strato-cumulus
10	Central Mid-Atlantic	10S-20S	26W-16W	Trade wind cumulus
11	Gough Island	39S-49S	16W- 6W	Storm track

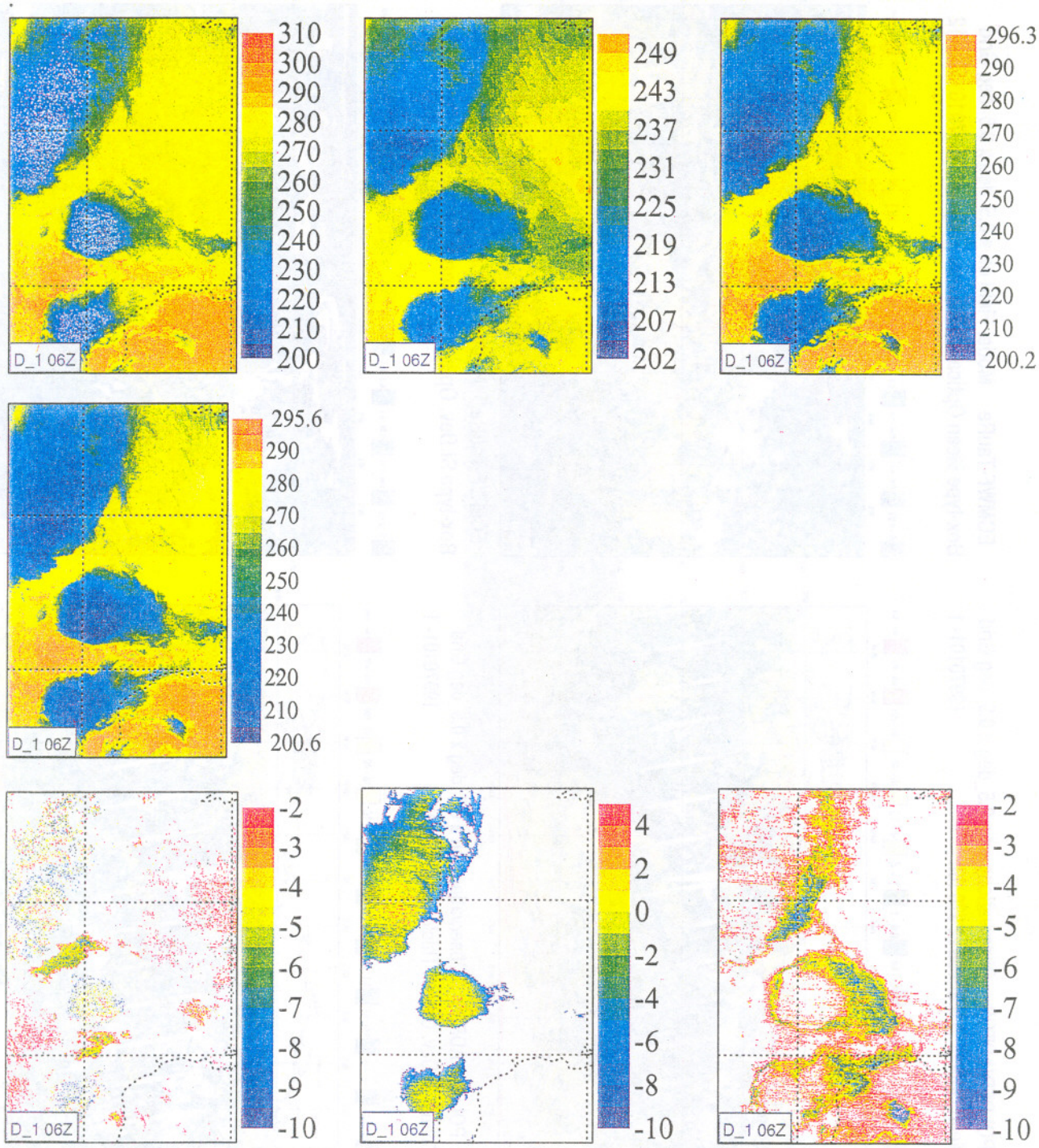

Figure 5: GOES-8 brightness temperatures for 20000401 06UTC over the ARM-SGP "GOES" area, in the different longwave channels (top left is 3.99 μm, top middle is 6.99 μm, top right is 10.6 μm, middle left is 11.5 μm). Bottom row presents the brightness temperature differences (bottom left is 3.99-10.6 μm, bottom middle is 6.99-10.6 μm, bottom right is 11.5-10.6 μm).

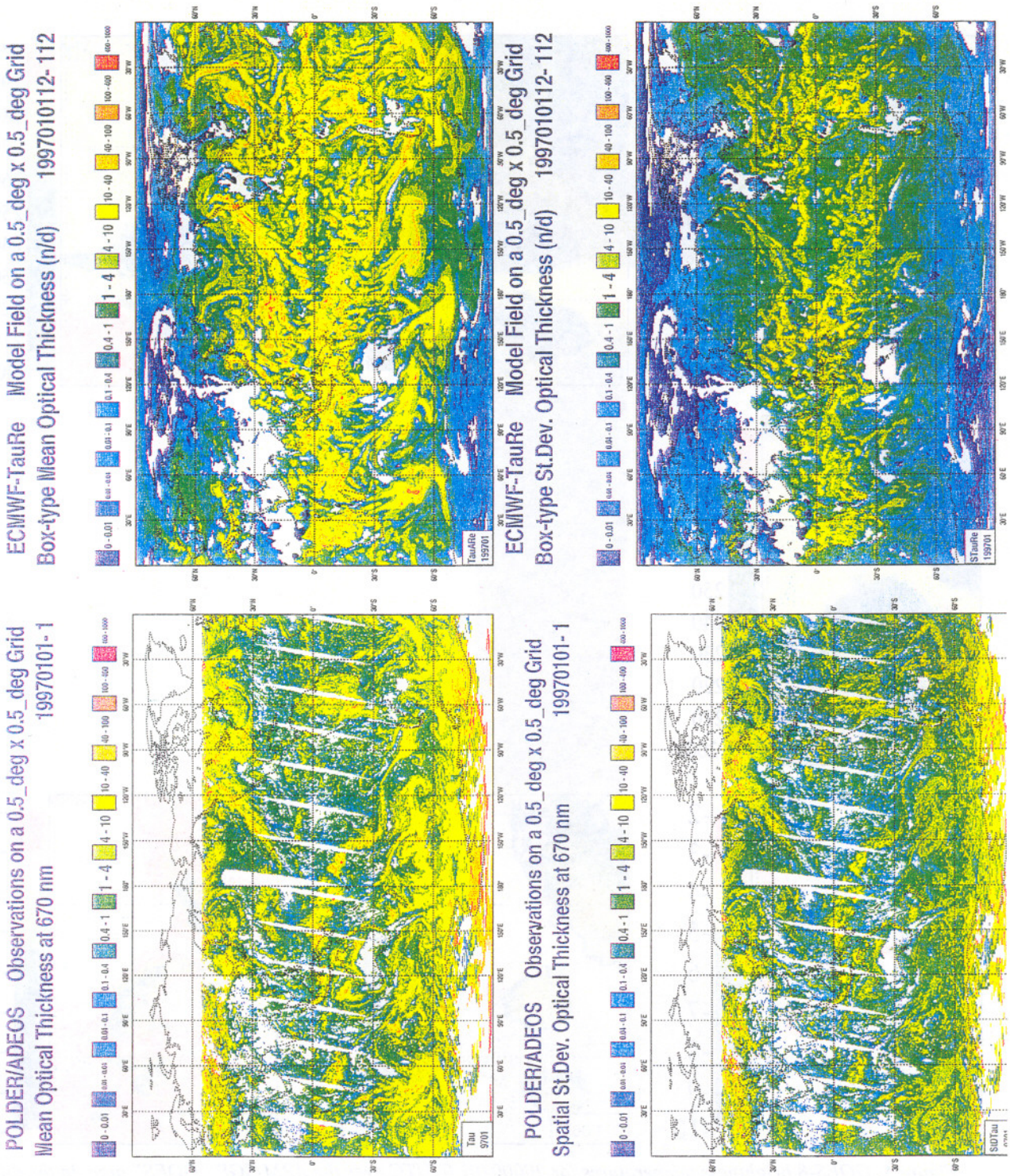

Figure 6: The cloud optical thickness at 670 nm (top) derived from POLDER (left) and the model visible optical thickness (right) for 19970101. Observation data arre plotted averaged over a 0.5 x 0.5 deg^2 grid. The model field is extracted from the 6-hour first-guess forecasts closest in time to the satellite pass and corresponds to a T213 resolution (0.5625 x 0.5625 deg^2).The corresponding spatial standard deviation of the optical thickness at 670 nm is presented at the bottom.It is computed from the indicidual 6 x 7 km^2 pixel for a grid of 0.5 x 0.5 deg^2.The spatial standard deviation of the model visible optical thicknessis computed using the box-type method of Jakob and Klein (2000)

4. Spectral dependence of radiances

The GOES-8 satellite carries four longwave channels at 3.9, 6.9, 10.9 and 11.5 μm. An example of the brightness temperatures seen in these channels is presented in Figure 5. In the past, various authors have discussed the potential of multi-spectral techniques to determine macroscopic cloud characteristics. Using a split channel technique on the two longwave window channels (10.5 and 11.5 μm) of AVHRR, *Inoue* (1985), *Wu* (1987) and *Parol et al.* (1991) could distinguish ice clouds from liquid water clouds and infer some information on the effective radius of the ice particles. A similar approach can be used with the various longwave channels from GOES-8. Figure 5 presents results from various combinations of channels that allow to delineate low-level clouds (ground fog?) from a difference between 3.9 and 10.6 μm, the deep core (unity emissivity) fraction of clouds from a difference between 6.9 and 10.9 μm, and the semi-transparent high clouds associated with the deep systems from a difference between 11.5 and 10.9 μm. Such information can be very useful to check some aspects of the model cloudiness. At present, we are unable to simulate such spectral signatures, due to the lack of account for the scattering of longwave radiation in the RTTOV-6 package, and/or to deficient model clouds, through an inadequate water loading, a wrong phase of water in the upper parts of the clouds, and/or an inappropriate representation of the longwave optical properties.

5. Spatial variability of shortwave optical thickness

The present version of the cloud scheme uses vertical distributions of the (grid-mean) temperature, humidity, and wind to provide the cloud fraction and cloud water. Similarly, the radiation scheme only uses these (grid-mean) cloud, temperature and humidity profiles to compute the radiative fluxes. Work by *Cahalan* (1994) and *Barker et al.* (1996, 1997) have shown that, even if a large-model is producing the correct distribution of the grid-mean cloud water, the sub-grid scale variability of this cloud water is an important parameter to take into account if proper radiative fluxes are to be computed. Observations of the cloud optical thickness with a horizontal resolution of [6 x 7 km^2] by ADEOS-POLDER (*Buriez et al.*, 1997) have been compared to the optical thickness produced by the cloud scheme in the operational forecast for January 1997. To get a proper comparison, and given the T213 horizontal resolution of the ECMWF model at the time (i.e., a grid of $[0.5625^o]^2$), we used the "box-type" method of *Jakob and Klein* (1999) within 81 sub-columns to determine within each model grid the spatial variability of the optical thickness. In this approach, each individual model grid is sub-divided into N sub-columns over which a cloud layer can only have a cover of zero or unity, and the total cloud optical thickness is computed for each sub-column by vertically integrating the layer cloud water amounts. Figure 6 compares the total cloud optical thickness and its spatial standard deviation (at roughly 60 km scale) from POLDER and derived from the model, for an ensemble of satellite orbits covering the globe on a given day (1 January 1997). The satellite information might not be relevant over the bright surfaces of Antarctica. This version of the model clearly overestimates the cloud optical thickness in the 30^oN-30^oS area, with model optical thickness in

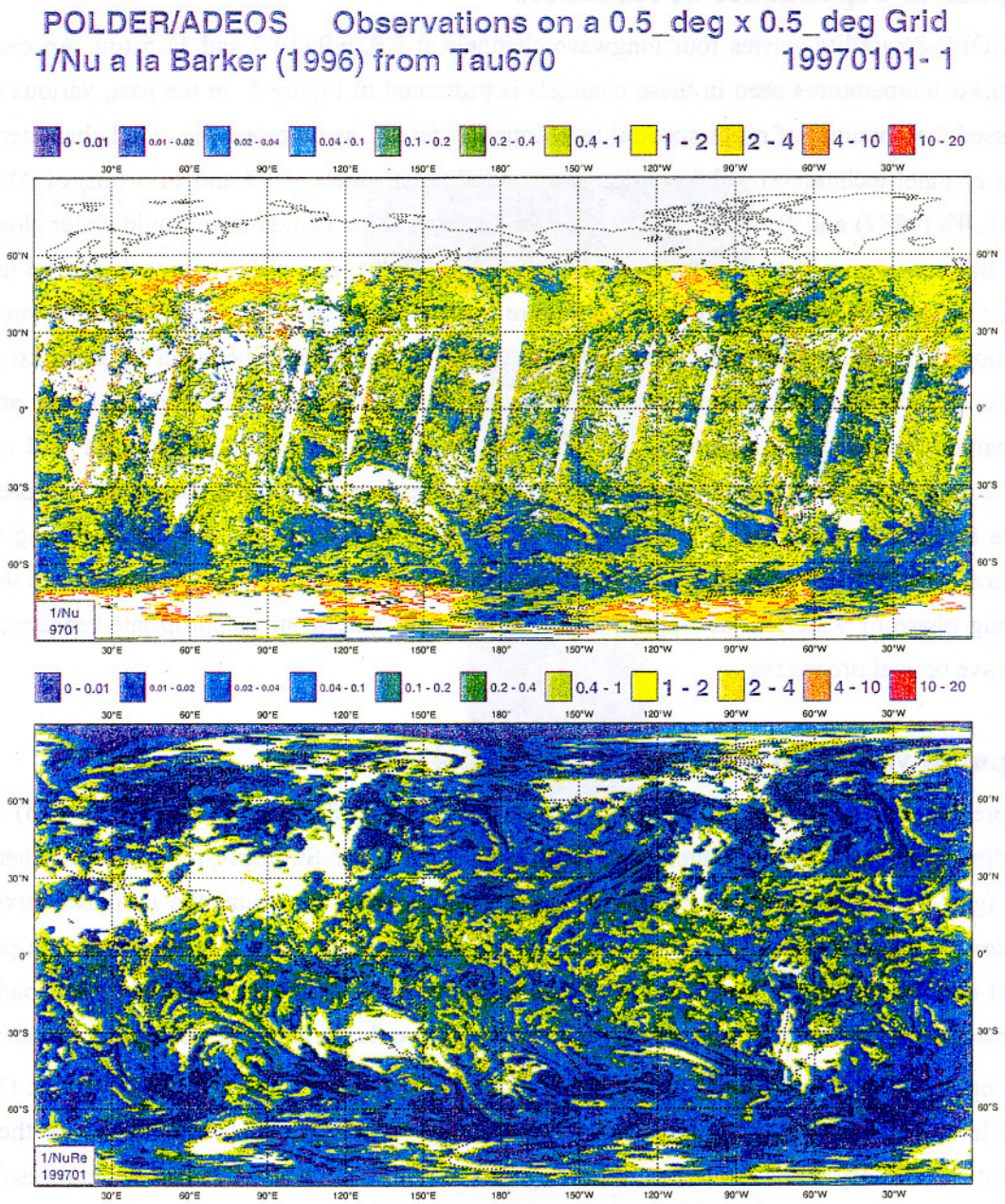

Fig 7: The inhomogeneity parameter a la Barker (1996) ($1/\nu = (\bar{\tau}/\sigma)^2$) from the cloud optical thickness of Fig 6.

excess of 100 where observations are usually in the 10 to 40 range. The model standard deviation is high only in the tropics and falls below 4 when going to mid-latitudes. The observations generally show lower values of $\sigma(\tau)$ in the tropics, but values of the same order of magnitude (between roughly 10 and 100) as τ in the mid-latitudes of the Northern Hemisphere. *Barker et al.* (1997) has recently proposed to correct for the effect of the model sub-grid scale spatial inhomogeneity in the distribution of the cloud water by

introducing a factor related to ν, the ratio of the standard deviation over the grid averaged cloud optical thickness. Figure 7 shows a comparison of such factors derived from both POLDER observations and the model. It is quite clear that the simple "box-type" approach outlined above is not sufficient for the representation of the spatial inhomogeneities.

5. Perspectives

In this short study, we show how some satellite data are used to check and validate the clouds and radiation fields produced by the ECMWF forecast model. In a weather forecast environment, stress is usually put on relatively short time and space scales for which the new generation of operational polar-orbiting (AMSU, and the forthcoming AIRS, IASI) and geostationary satellites (i.e., GOES-8, but also GMS-5, and MSG in the coming years) offers observations allowing to build more stringent tests on the model representation of the cloud-radiative processes, particularly with respect to the life cycle of cloudiness, diurnal evolution of semi-tropical and tropical cloudiness. Observations from experiments on other research satellites (i.e., ADEOS-POLDER, but also CERES, MODIS) can also offer new avenues for verifying the model behaviour. The challenge is to find new and better ways of exploiting this information to first invalidate, then improve the model.

References

Barker, H.W., B.A. Wielicki, and L. Parker, 1996: A parameterization for computing grid-averaged solar fluxes for inhomogeneous marine boundary layer clouds. Part II: Validation. J. Atmos. Sci., 53, 2304-2316.

Barker, H.W., and B.A. Wielicki, 1997: A parameterization of grid-averaged longwave fluxes for inhomogeneous marine boundary layer clouds. J. Atmos. Sci., 54, 2785-2798.

Buriez, J.-C., C. Vanbauce, F. Parol, P. Goloub, M. Herman, B. Bonnel, and Y. Fouquart, 1997: Cloud detection and derivation of cloud properties from POLDER. Int. J. Remote Sensing, 18, 2785-2813.

Cahalan, R.F., 1994: Bounded cascade clouds: Albedo and effective thickness.Nonlin. Proc. Geophys., 1, 156-167.

Chaboureau, J.-P., J.-P. Cammas, P. Mascart, J.-P. Pinty, C. Claud, R. Roca, and J.-J. Morcrette, 2000: Evaluation of a cloud system life-cycle simulated by Meso-NH during FASTEX using METEOSAT radiances and TOVS-3I cloud retrievals. Q. J. Roy. Meteor. Soc., in press.

Chevallier, F., et al., 2000: Comparison between satellite observations and the ECMWF model in presence of clouds. ECMWF Research Department Memo. R43.8/FC/37, 8 pp.

Chevallier, F., and J.-J. Morcrette, 2000: Comparison of model fluxes with surface and top-of-the-atmosphere observations. Mon. Wea. Rev., 128, 3839-3852.

Duvel, J.-Ph., and R.S. Kandel, 1985: Regional-scale diurnal variations of outgoing infrared radiation observed by METEOSAT. J. Climate Appl. Meteor., 24, 335-349.

Ellingson, R.G., and R.R. Ferraro, 1983: An examination of a technique for estimating the longwave radiation budget from satellite radiance observations. J. Clim. Appl. Meteor., 22, 1416-1423.

Ellingson, R.E., Hai-Tien Lee, D. Yanuk, and A. Gruber, 1994: Validation of a technique for estimating outgoing longwave radiation from HIRS radiance observations. J. Atmos. Ocean. Technol., 11, 357-365.

Inoue, T., 1985: On the temperature and effective emissivity determination of semi-transparent cirrus clouds by bi-spectral measurements in the 10 micrometer window region. J. Meteor. Soc. Japan, 63, 88-96.

Jakob, C., 1999: Cloud cover in the ECMWF reanalysis. J. Climate, 12, 947-959.

Jakob, C., and S.A. Klein, 1999: The role of vertically varying cloud fraction in the parametrization of microphysical processes in the ECMWF model. Quart. J. Roy. Meteor. Soc., 125A, 941-965.

Jakob, C., and S.A. Klein, 2000: A parametrization of the effects of cloud and precipitation overlap for use in general circulation models. Quart. J. Roy. Meteor. Soc., 126C, 2525-2544.

Klein, S.A., and C. Jakob, 1999: Validation and sensitivities of frontal clouds simulated by the ECMWF model. Mon. Wea. Rev., 127, 2514-2531.

Mahfouf, J.-F., and F. Rabier, 2000: The ECMWF operational implementation of four dimensional variational assimilation: Part II: Experimental results with improved physics. Quart. J. Roy. Meteor. Soc., 126A, 1171-1190.

Mlawer, E.J., S.J. Taubman, P.D. Brown, M.J. Iacono, and S.A. Clough, 1997: Radiative transfer for inhomogeneous atmospheres: RRTM, a validated correlated-k model for the longwave. J. Geophys. Res., 102D, 16,663-16,682.

Morcrette, J.-J., 1990: Impact of changes to the radiation transfer parameterizations plus cloud optical properties in the ECMWF model. Mon. Wea. Rev., 118, 847-873.

Morcrette, J.-J., 1991: Evaluation of model-generated cloudiness: Satellite observed and model-generated diurnal variability of brightness temperature. Mon. Wea. Rev., 119, 1205-1224.

Parol, F., J.-C. Buriez, G. Brogniez, and Y. Fouquart, 1991: Information content of AVHRR channels 4 and 5 with respect to the effective radius of cirrus cloud particles. J. Appl. Meteorol., 30, 973-984.

Rabier, F., H. Jarvinen, E. Klinker, J.-F. Mahfouf, and A. Simmons, 2000: The ECMWF operational implementation of four dimensional variational assimilation: Part I: Experimental results with simplified physics. Quart. J. Roy. Meteor. Soc., 126A, 1143-1170.

Raisanen, P., 1998: Effective longwave cloud fraction and maximum-random overlap of clouds: A problem and a solution. Mon. Wea. Rev., 126, 3336-3340.

Rikus, L., 1997: Application of a scheme for validating clouds in an operational global NWP model. Mon. Wea. Rev., 125, 1615-1637.

Rizzi, R., 1994: Raw HIRS/2 radiances and model simulations in the presence of clouds. ECMWF Technical Report No. 73, 29 pp, September 1994.

Roca, R., L. Picon, M. Desbois, H. Le Treut, and J.-J. Morcrette, 1997: Direct comparison of Meteosat water vapor channel data and general circulation model results. Geophys. Res. Letters, 24, 147-150.

Saunders, R.W., M. Matricardi, and P. Brunel, 1999: An improved fast radiative transfer model for assimilation of satellite radiance observations. Quart. J. Roy. Meteor. Soc., 125, 1407-1425.

Slingo, J.M., 1987: The development and verification of a cloud prediction scheme for the ECMWF model. Quart. J. Roy. Meteor. Soc., 113, 899-928.

Tiedtke, M., 1993: Representation of clouds in large-scale models. Mon. Wea. Rev., 121, 3040-3061.

van den Hurk, B.J.J.M., P. Viterbo, A.C.M. Beljaars, and A.K. Betts, 2000: Offline validation of the ERA40 surface scheme. ECMWF Technical Memo. No. 295, 42 pp.

Washington, W.M., and D.L. Williamson, 1977: A description of the NCAR GCMs. "GCMs of the atmosphere". J. Chang, Ed., Methods in computational physics, Vol. 17, Academic Press, 111-172.

Wu, M.-L., 1987: Determination of cloud ice water content and geometrical thickness using microwave and infrared radiometric measurements. J. Climate Appl. Meteor., 26, 878-884.